Influence of ENSO and the Atlantic multi-decadal Oscillation on Drought over the United States

Kingtse C. Mo, Jae-Kyung E. Schemm and Soo-Hyun Yoo

Climate Prediction Center/NCEP/NWS

December 2008

Corresponding author: Kingtse C. Mo, Climate Prediction Center/NCEP
NWS/NOAA, 5200 Auth Rd., Camp Springs, Md 20746
Email: kingtse.mo@noaa.gov

Abstract

Composites based on observations and model outputs from the CLIVAR drought experiments were used to examine the impact of El Nino Southern Oscillation (ENSO) and the Atlantic multi-decadal oscillation (AMO) on drought over the United States. The experiments were performed by forcing an AGCM with prescribed sea surface temperature anomalies (SSTAs) superimposed on the monthly mean SST climatology. Four model outputs from the NCEP GFS, NASA NSIPP1, GFDL AM2.1 and LDEO/NCAR CCM3 were analyzed in this study.

The impact of ENSO on drought over the United States is concentrated over the Southwest, the Great Plains and the lower Colorado River Basin with cold (warm) ENSO events in favor of drought (wet spells). Over the East Coast and the Southeast, the impact of ENSO is small because the precipitation responses to ENSO are opposite in sign for winter and summer. For these areas, a prolonged ENSO from winter to summer does not favor persistent drought or wet spell.

The direct influence of the AMO on drought is small. The major influence of the AMO is to modulate the impact of ENSO on drought. The influence is large when the SSTAs in the tropical Pacific and in the North Atlantic are opposite in phase. A cold ENSO event in a positive AMO phase favors drought over the Southwest, the Great Plains and the Colorado River basin. A warm ENSO event in a negative AMO phase has the opposite impact. The ENSO influence on drought is much weaker when the SSTAs in the tropical Pacific and in the North Atlantic are in phase.

1. **Introduction**

Long lasting drought has enormous impact on the nation's economy and society. Better drought prediction can mitigate devastating economic effects on people and ecosystems. To improve drought forecasts, one needs to understand the causes that trigger and sustain drought. Because drought implies prolonged rainfall and soil moisture deficits, they are often modulated by low frequency sea surface temperature anomalies (SSTAs). In the Pacific, decadal trends of SSTAs in the North Pacific and the tropical Pacific can influence the drought occurrence over the United States (Mo and Schemm 2008a, Dai et al. 2004).

In the Atlantic, the Atlantic Multi-decadal Oscillation (AMO) mode has been linked to rainfall and river flow anomalies over the United States. The AMO is defined as the first rotated Empirical Orthogonal Function (EOF) of non-ENSO SSTAs, but the associated PC is highly correlated to the mean Atlantic SSTAs from the Equator to 60 ^{o}N (Mestas-Nunez and Endfield 1999). The warm (cold) phase of the AMO is associated with less (more) rainfall over the Mississippi basin and more (less) streamflow over the Lake Okeechobee in Florida (Enfield et al. 2001). McCabe et al. (2004) correlated 20-yr moving drought frequency with 20-yr AMO time series. They found that the warm (cold) phase of the AMO is associated with more (less) frequent drought occurrence over the Southwest, the north central United States and less (more) drought events over Florida. Schubert et al. (2004) identified the Atlantic SSTAs as contributors to droughts over the Great Plains.

In the interannual frequency band, ENSO has large influence on the occurrence of drought (Ropelewski and Halpert 1986, 1989, Dai et al. 1998, Mo and Schemm

2008a). Barlow et al. (2001) attributed the North Pacific SSTAs and ENSO to summer droughts over the United States. Many studies have suggested that the influence of ENSO on drought is modulated by the AMO. For example, Endfield et al. (2001) found that the ENSO impact on winter rainfall depends on the phase of the AMO. Rogers and Coleman (2003) found that interactions between the AMO and the Pacific teleconnection modes modulate the Mississippi streamflow in winter. Different phases of the AMO also link to different summer precipitation modes of the North American monsoon (Hu and Feng 2008).

Over the United States, the observed precipitation (P) and SST data (Smith et al. 1996) cover less than 150 years. These data sets do not cover enough AMO cycles to get robust statistics for diagnostic studies. One possibility is to rely on AGCM experiments to confirm observational findings. The AGCM experiments designed by the United States CLIVAR (USCLIVAR) drought working group (Schubert et al. 2008) are well suited for this purpose. The drawback of model experiments is that all models have non systematic errors. These errors can not be corrected by the climatology run in which the AGCM is forced by the climotological SSTs. Therefore, both observations and model experiments are needed to study the precipitation and atmospheric responses to the low frequency SSTA forcing.

The purpose of this paper is to examine the impact of (a) ENSO, (b) the AMO and (c) the combinations of the different phases of the AMO and ENSO on drought over the United States. We draw our conclusions from composites based on observations and model simulations from the USCLIVAR experiments. The observational data sets and a brief description of the USCLIVAR experiments are outlined in section 2. The influence of ENSO on drought is discussed in section 3. The impact of the decadal AMO on drought is presented in section 4 and the indirect influence of the AMO on drought through ENSO is given in section 5. Discussions are given in section 6.

2. Data and Experiments

a) Data

The monthly mean precipitation (P), soil moisture and runoff data sets were obtained from the North American Land Data Assimilation system (NLDAS) Variable Infiltration Capacity (VIC) model outputs from the University of Washington. The data set covers the period 1915-2006. The P is based on the cooperative observer station meteorological daily data with the Precipitation Regression on Independent Slopes Method (PRISM) correction (Maurer et al. 2002). The differences between the monthly mean P anomalies from this data set and from the CPC unified gauge based P analysis (Higgins et al. 2000) for the overlapping period 1950-2006 is small. From P, we calculated the 6-month Standardized Precipitation Index (SPI6) *(*Hayes et al. 1999, Mckee et al. 1993, 1995). The SPI6 measures the P deficit or wetness for the past 6 months. In addition to SPI, soil moisture percentiles and runoff anomalies are also used to represent different aspects of drought (Mo 2008). Runoff was used to compute the standardized runoff index that is the same as the SPI, but runoff is used instead of precipitation (Shukla and Wood 2008, Mo 2008). A drought (wet) event is defined as the SPI6 index or the SRI6 index being less than -0.8 (greater than 0.8) or the soil moisture percentile being less (more) than 20% (Svoboda et al. 2002).

The SST data are the monthly reconstructed SSTs from Smith et al. (1996) updated to 2006. The data set covers the base period 1915- 2006. The horizontal resolution is 2^{o} . Climatological monthly means for the base period are removed from each data set to obtain anomalies.

The ENSO pattern is represented by the first mode of the annual mean global SSTAs (Fig.1a). It shows positive SSTAs extending from the central to the eastern Pacific with negative SSTAs in the North and South Pacific. The AMO is represented by the first mode of SSTAs over the Atlantic (Fig.1b). It shows a horseshoe shape pattern with positive SSTAs over the North Atlantic from 60-75 ^{o}N and over the tropical North Atlantic. This mode resembles the first non-ENSO mode (Mestas-Nunez and Endfield 1999). The decadal variations of the associated PC resemble the AMO. According to Endfield et al (2001), Hu and Feng (2008) and McCabe et al. (2004), the warm phase of the AMO covered the periods 1930-1959, 1995-2006 while the cold phase covered the periods 1915-1925 and 1965-1990.

Composites are used to study the influence of ENSO, the AMO and the combinations of the two modes on drought over the United States. The seasonal mean SSTAs for winter (January-March; JFM), spring (April- June; AMJ), summer (July-September; JAS) and autumn (October-December; OND) were projected onto the REOF 1 (Fig.1a) or the Atlantic REOF 1 (Fig.1b) to obtain the rotated principal component RPC. Warm (cold) events were selected when RPC was great than 1 (less than -1) standard deviation. Composites of P and SPI6 were obtained for positive and negative RPC events separately. The results are displayed as the differences between cold and warm events.

To test the statistical significance of a composite map from observations or the frequency of the drought occurrence from a model experiment, the Monte Carlo method was used (Mo and Schemm 2008b). We use the composite of P as an example to outline the method. Composites were computed from randomly selected maps from the same P time series. The process was repeated 500 times. The statistical significance of the tested map can be determined from these 500 cases at each grid point. The anomaly composite should be within 5 percentiles of the distribution function determined by composites of randomly selected maps. The areas in which values of the composite field are statistically significant at the 5% level are shaded. The composites of SPI6 or the frequency of drought occurrence can be tested the same way.

b) USCIVAR SST experiments

The GCM experiments were designed by the USCLIVAR drought working group to study the relationships between persistent SST forcing and drought. The ENSO pattern (Fig.1a) is labeled as P. The Atlantic pattern (Fig.1b) is labeled as A. Different experiments were carried out by forcing the AGCM with SST boundary conditions in combinations of these two modes.

Positive or negative anomalies associated with the warm (w) phase and the cold (c) phase of each pattern were added to the SST monthly mean climatology to form a global SST distribution to force the AGCM (Schubert et al. 2008). The monthly mean climatology is labeled as neutral (n). The experiment forced by the monthly mean climatology is labeled as PnAn. The experiments with the combinations of the Pacific or the Atlantic anomalies (Fig.1) are labeled as PxAy, where x is labeled as c for cold, w for warm and n for neutral SSTAs in the Pacific. Similarly, y denotes the SSTAs in the Atlantic. For example: the experiment forced by cold (warm) SSTAs in the Pacific but no SST anomalies in the Atlantic is labeled as PcAn (PwAn). The experiment forced by warm (cold) SSTAs in the Atlantic but no anomalies in the Pacific is labeled as PnAw (PnAc).

We analyzed 9 experiments: PnAn, PwAn, PcAn, PnAw, PnAc, PcAc, PcAw, PwAc, and PwAw from the NCEP (GFS) (Campana and Caplan 2005), NASA (NSIPP1) (Bacmeister et al. 2000, Schubert et al. 2004), GFDL (AM2.1) (Delworth et al. 2006, Milley et al. 2002) and the LDEO/NCAR (CCM3) (Kiehl et al. 1998, Seager et al. 2005). They are labeled as the GFS, NSIPP, GFDL and CCM3 experiments respectively. Each GFS experiment lasts only 36 years. The NSIPP and the GFDL experiment last for 50 years and the CCM3 experiment lasts for 51 years. P and 200 hPa height monthly means were extracted from each run.

The GFS is used as an example to describe the procedures used to calculate the frequency of drought occurrence and anomalies. We pooled P from 9 experiments together to form a time series of 36x12x9 months. The climatological monthly means (grand means) can be calculated each month from this pooled time series. They are similar to the climatological monthly means calculated from the PnAn experiment. For each experiment, monthly mean anomaly is the departure from the grand monthly mean for that month.

The 6-month SPI6 was calculated from the pooled time series of monthly mean anomalies and the SPI6 for the first year of each experiment was discarded. For each experiment, the frequency of drought occurrence was determined by counting the number of month (num) that the SPI6 is below -0.8 at each grid point. Because each experiment has different length of integration, the frequency of occurrence is given as the ratio between num and the total length of the experiment. For the GFS, the length is 35x12. The statistical significance was assessed by the Monte Carlo method. For each experiment, the ensemble mean of any variable was obtained by taking the equally weighted mean of that variable from the GFS, NSIPP, CCM3 and GFDL model runs.

3. Impact of ENSO on drought over the United States

a) Observations

From P and SPI6 time series, composites of positive and negative events were obtained for each season based on the RPC associated with Fig. 1a. They are presented as the differences between negative (cold) and positive (warm) events (Fig. 2). The P responses to ENSO are seasonally and regionally dependent (Figs. 2e-2h). The responses to a cold ENSO winter are negative P anomalies over the Southwest, California, the Great Plains, the Southeast, the East coast from Florida to 40 ^{o}N and positive P anomalies over the Pacific Northwest and the Ohio Valley. The P anomalies for the spring composite are small. For JAS, a cold ENSO event is likely associated with positive P anomalies over the East Coast and the Southeast, and negative anomalies over the north central United States. For OND, negative anomalies are located over the eastern United States east of 100 ^{o}W except the Northeast and the Southwest with positive anomalies over the Pacific Northwest. The cold (warm) ENSO events favor dryness (wetness) for the Southwest and the Great Plains for all seasons. If a cold (warm) ENSO event persists for many seasons, dry (wet) conditions over these regions are likely to persist. However, the situation is very different for the East Coast and the Southeast where the P responses to ENSO for winter and summer are opposite in phase. For these regions, a perpetual ENSO does not favor persistent drought or wet spells (Mo and Schemm 2008b).

This point can be illustrated by the SPI6 composites that measure the occurrence of persistent drought or wet spells (Figs. 2a-2d). The SPI6 for JFM is contributed by P anomalies in OND and JFM. It shows that drought is more likely to occur over the Southeast, Southwest, Florida and the Great Plains and wet spells are like to occur over the Pacific Northwest during cold ENSO events. The composite for AMJ is similar to JFM except it shows wetness over the Ohio Valley. The composite for JAS is weak. The OND composite shows dryness over the Southwest, the Colorado basin and the north central United States. For warm events, the situation reverses.

In addition to SPI6, soil moisture and runoff indices have also been used to represent hydrological and agricultural droughts (Mo 2008). The composites for soil moisture anomalies and the 6-month standardized runoff index (SRI6) were obtained the same way as the SPI6 composite. The composites (Fig. 3) for all seasons together show that a cold (warm) ENSO favors drought (wetness) over the Great Plains and the Southwest. In contract, there is no strong signal over the East coast, the Southeast and the Ohio Valley. The seasonal cycles of P for these regions are weak (Mo and Schemm 2008a). Therefore, P anomalies for many seasons can contribute to long term measures of drought such as SPI6. Because the P responses to ENSO are opposite in phase for winter and summer and an ENSO event tends to last more than one season, the SPI6 composite (Fig. 3) does not show any significant signal over these areas. The large differences between P and SPI6 composites illustrate that drought means *persistent* P deficits.

b) Model experiments

The frequency of drought occurrence is presented as the ratio of number of months with SPI6 < -0.8 and the total length of a given experiment. To examine the influence of ENSO on drought, we presented the frequency of drought occurrence for the experiment PwAn (warm Pacific with no Atlantic forcing) and PcAn (cold Pacific with no Atlantic forcing) for each model separately (Fig. 4) and the multi- model ensembles (Figs. 5a and 5e). Results are summed up as follows:

1. The multi-model ensemble means are consistent with the composites based on observations (Fig. 3). The warm Pacific SSTAs (PwAn) favor less drought events (Fig. 5a) over the Southwest and the lower Colorado River basin, and the Great Plains with a minimum over Texas. The ENSO has very little influence on drought over the eastern United States. The PcAn has the opposite impact (Fig. 5e).
2. While the multi –model ensemble compares favorably with the ENSO composites from observations (Fig. 3a), there are large variations from one model to another (Fig. 4). Not every model simulation agrees with the observations. Models compensate one another and the multi model ensemble has the most reliable results.
3. The GFS, NSIPP and GFDL runs all capture the west-east contrast, but they differ in spatial details. The GFDL runs show that the impact of ENSO extends to 85^{o}W while the impact is limited to the west of 90^{o}W for the GFS runs. Both the CCM3

and the NSIPP runs show the largest impact of a perpetual ENSO over the central United States and the Southwest. The CCM3 runs indicate that the influence of ENSO extends to the east coast and signals over the Colorado River basin are too weak.

To examine the evolution of the model runs, we plotted the time series of P averaged over the Great Plains (32-40 ^{o}N, 90-105^{o}W) and the Southeast (32-40^{o}N 75-80^{o}W land points) for winter (December –March, red line), summer (June-September, Green line) and the entire year (dark circles) for each model (Fig. 6). P averaged over the Great Plains (Figs. 6a-6h) settles into a regime after a period of spin up. All models show positive anomalies for PwAn experiment and negative anomalies for PcAn. The P responses over the Great Plains are not seasonally dependent. For GFS, CCM3 and GFDL runs, both summer and winter P contribute to drought (wet spells). The NSIPP runs show large responses in summer and very weak anomalies in winter.

For the Southeast (Fig. 6i-6p), the situation is very different. The GFS and GFDL models capture the phase reversal between winter and summer responses to ENSO so the net responses are small. The NSIPP model has no response in winter and small contributions are from summer rainfall. The CCM3 model captures the phase reversal between summer and winter, but the response for winter is stronger than summer so the annual response to PwAn (PcAn) is positive (negative).

To show the P response to ENSO over the United States, the P climatological means averaged over the last 25-years of a given experiment for summer and winter are calculated. This was done to avoid spinup. Fig. 7 shows the differences of the climatological P means between PwAn and PcAn experiments. Both the GFS and the GFDL runs capture the ENSO influence on P reasonably well in comparison with observations (Fig. 2). Although, the GFS model misses the negative P anomalies over the Pacific Northwest and the GFDL model does not capture the negative P anomalies over the Ohio Valley in winter. Both models did not capture negative anomalies over the east coast in summer. The NSIPP runs have very weak response in winter and summer anomalies over the Great Plains are too strong. For the CCM3 runs, the response over the western region is too weak and the center of the maximum summer rainfall shifts too far south. The models have large precipitation errors. However, the multi model ensembles preserve the primary responses to the SST forcing. This also confirms the findings of Palmer et al. (2004) that the multi model ensemble gives superior results than individual model runs.

Based on the model ensembles and composites from observations, we conclude that the largest impact of ENSO on drought is over the Southwest, the lower Colorado Basin, and the Great Plains with cold ENSO events favoring droughts. The ENSO influence on drought over the eastern United States including the East Coast and the Southeast is small because the P responses to ENSO for winter and summer are opposite in phase.

4) Influence of the Atlantic SSTAs on drought

(a) Observations

To study the impact of the Atlantic SSTAs on drought over the United States, the positive and negative cases were selected from the RPC associated with the Atlantic pattern (Fig. 1b). The composite difference of SPI6 between positive and negative events with all seasons together (Fig. 8b) shows very weak anomalies. There is no value below -0.8. This suggests that there is no statistically significant signal in the non-filtered data. The influence of the Atlantic SSTAs on drought in the interannual band is small.

To study the decadal influence of the Atlantic forcing, the P composite differences between positive phase (1930-1959, 1995-2006) and negative phase (1915-1925, 1965-1990) of the AMO were plotted for winter (Fig. 8a) and summer (Fig. 8e). The winter composite shows negative P anomalies over the Southeast except Florida and positive anomalies over the West Coast north of 38^{o}N and the area extending from eastern Texas northeastward to the Ohio Valley. The summer composite (Fig. 8e) shows positive anomalies over Florida and negative anomalies over the North Central. The anomalies are statistically significant at the 10% level but the magnitudes are very small. They are only about 0.2 mm day^{-1}. The SPI6 composite difference between warm and cold phase of the AMO for all seasons together (Fig. 8f) has coherent negative anomalies over the Southwest, but values are only around 0.2 This suggest that the AMO may create favorable background flow for drought or wet spells to occur, but the direct influence on drought is limited. When data are filtered for the decadal frequency band, the correlations may be statistically significant. However, the decadal AMO does not contribute to large percentage of variances. Therefore, the total direct influence on drought for the AMO is weak. This is also confirmed by the model experiments.

b) Model experiments

The experiments PnAw and PnAc can be interpreted as the atmospheric responses to the decadal warm (PnAw) and cold (PnAc) AMO forcing. The frequency of drought occurrence for the multi model ensemble for PnAw and PnAc are given in Figs. 5b and 5f respectively. They show that drought is more likely to occur over New Mexico for the warm phase of the AMO. For the cold phase of the AMO, the response is very weak. There is also large spread among different model runs (not shown).

In conclusion, both model and observational results show that the direct influence of the AMO or the Atlantic forcing on drought over the United States is very weak and is mostly confined to the Southwest.

5) Modulation of the AMO on the ENSO influence on drought

While the direct impact on drought is small, the AMO can modulate the impact of ENSO or other teleconnections on P over the United States (Endfield et al. 2001, Rogers and Coleman 2003). In this section, we examine the modulation of the impact of ENSO on drought by the AMO.

a) Observations

To examine the impact of ENSO and AMO together, composites of SPI6 for cold and warm ENSO events based on RPC 1 (Fig. 1) for all seasons together were computed for the positive and negative decades of AMO separately. The statistical significance is assessed based on the Monte Carlo test.

The influence of ENSO on drought is large when the tropical Pacific and the Atlantic SSTAs are opposite in phase (Figs. 8c and 8h). For the positive AMO and cold ENSO (Fig. 8c), drought is favored over the Southwest, the Colorado Basin, the

Great Plains, the East coast and the Southeast. For the negative AMO and warm ENSO (Fig. 8h), wetness is more likely to occur over approximately the same areas except the Southeast where the signal is weaker.

When the tropical Pacific and the Atlantic SSTAs are in phase, the net impact on drought is weak (Figs. 8d and 8g). The statistical significant signals are found over the southern Plains and the Southwest, but the magnitudes are smaller. Overall, results are consistent with Endfield et al. (2001) except that their composites of P are for winter season.

b) Model experiments

The observational results (Fig. 8) indicate while the direct impact of the AMO on drought is small, it modulates the impact of ENSO on droughts. Because the length of the observational data sets only covers less than 2 cycles of the AMO, model experiments can be used to substantiate the findings.

The spread of the frequencies of drought occurrence among four models is very large for experiments with the combined Pacific and Atlantic SSTAs. Examples are given in Fig.9 for PcAc and PcAw. The multi model ensembles are given in Fig. 5c for PwAc, Fig. 5d for PwAw, Fig. 5g for PcAw and Fig. 5h for PcAc. Together with composites from observations (Fig.8), we can sum up the findings as fellows:

1. Both model and observations indicate that the influence of ENSO on drought over the United States is modulated by the AMO. The influences are greater when the SSTAs in the Pacific and the Atlantic are opposite in phase (PcAw and PwAc). The influence is much weaker when SSTAs in two basins are in phase (PcAc and PwAw).

2. All models and the ensemble mean show that there is a better chance for drought to occur over the Southwest, the Colorado River Basin and the Great Plains for PcAw. For PwAc, more wetness is favored over the about same areas. The areas of largest uncertainties are located over the East Coast and the Southeast where the model and observations do not agree and the spreads among models are large. For example, the model ensemble mean for PcAw shows no signal over the Southeast, but the composite shows dryness over the Southeast (Fig. 8c).

It is difficult to examine the circulation anomalies associated with such modulation based on observations. The NCEP-NCAR reanalysis starts from 1948 and the data set is not long enough (one AMO cycle) to obtain robust results. Prior to 1948, there were very limited observations available to obtain reliable objective analysis. Because the GFS model is able to capture the major features of the AMO and ENSO, we will use the GFS experiments to examine the circulation anomalies associated with the indirect influence of the AMO on drought through ENSO. We will use winter as an example because the responses of circulation anomalies are stronger. The monthly mean climatology was obtained by pooling all 9 experiments together.

For cold ENSO events without the influence of the AMO (PcAn), the circulation responses are a negative anomaly couplet straddling the equator over the cold SSTAs in the tropical Pacific and a Pacific North American type of the wave train with positive height anomalies close to the west Coast and negative anomalies extending from Canada to the Atlantic (Fig. 10c). The largest responses to the Atlantic SSTAs are in the North Atlantic with negative (positive) anomalies over cold (warm) water (Figs. 10a and 10f). For PnAc, there are positive height anomalies over the western

United States and negative anomalies over the northeastern Canada. For PnAw, there is a three cell pattern of height anomalies with negative anomalies extending to the east coast of the United States (Fig. 10f). For PcAw and PcAc, both the Atlantic SSTAs and the tropical Pacific SSTAs have impact on circulation and precipitation anomalies. For PcAc, the net influence is that positive anomalies extend more inland from the North Pacific into the western United States with positive anomalies over the East Coast (Fig. 10e). Therefore, the PcAc has negative rainfall anomalies over the western United States and weak responses over the eastern part of the United States (Fig. 10d). For PcAw, anomalies over the United States are similar to PcAn. Therefore, rainfall pattern is also similar to the cold ENSO composite (Fig.2). The influence of the AMO is to modify the circulation responses to ENSO over the United States. That in turn modifies the P anomalies.

6. Conclusions

The influence of ENSO and the AMO on drought over the United States is examined using both composites from observations and the model experiments designed by the USCLIVAR drought working group. Different experiments were performed by forcing an AGCM with the combinations of the Atlantic (Fig. 1b) and ENSO (Fig. 1a) SSTAs superimposed on the monthly mean climatological SSTs (Schubert et al. 2008).

Because drought implies persistent dryness, the 6-month SPI is adopted to represent drought. The P composites are very different from the SPI composite. It is needed to recognize the importance of persistence in the studies of drought. The models respond differently even though they have the same forcing. However, the multi-model ensemble compares favorably with observations. This confirms conclusions in many studies that multi model ensemble is more reliable than single model results even for long term simulations (Palmer et. al 2004, Rowell 1988).

From both model simulations and observations, we conclude:

1. The impact of ENSO on drought over the United States is over the Southwest, the Great Plains and the lower Colorado River Basin with cold ENSO in favor of drought. Over the East Coast and the Southeast, the impact of ENSO is not large because the P responses to ENSO are seasonally dependent and opposite in sign for winter and summer. For these areas, a prolonged ENSO from winter to summer does not favor a persistent drought or wet spell.
2. The direct influence of the AMO on drought is small. There are suggestions that drought is more likely to occur over the Southwest but the anomalies are weak.
3. The major influence of the AMO is to modulate the impact of ENSO on drought. The influence is large when the SSTAs in the tropical Pacific and in the North Atlantic are opposite in phase. The cold ENSO in a positive AMO phase (PcAw) favors drought over the Southwest, the Colorado River basin and the Great Plains. The warm ENSO in a negative AMO phase (PwAc) has the opposite impact. There are large uncertainties of the influence of the AMO and the ENSO over the Southeast and the East coast. The model simulations have large spread and they do not agree with observations.

Acknowledgements

This work was carried out as a part of a U. S. CLIVAR drought working group activity supported by NASA, NOAA and NSF to coordinate and compare climate model simulations forced with a common set of idealized SST patterns. The authors would like to thank NASA's Global Modeling and Assimilation Office (GMAO) for making the NSIPP1 runs available, the Lamont-Doherty Earth Observatory of Columbia University for making their CCM 3 runs available, NOAA's Climate Prediction Center (CPC) Climate Test Bed (CTB) for making the GFS runs available, NOAA's Geophysical Fluid Dynamics Laboratory (GFDL) for making the AM2.1 runs available, the National Centers for Atmospheric Research (NCAR) for making the CAM 3.5 runs available and the Center for Ocean Land Atmosphere (COLA) and the University of Miami's Rosenstiel School of Marine and Atmospheric Science for making the CCSM3.0 coupled model runs available. This project is supported by the CPPA grant GC06-012.

References:

Barlow, M, S. Nigam and E. H. Berbery, 2001: ENSO, Pacific decadal variability and the US summertime precipitation drought and streamflow. *J. Climate*, **14**, 2105-2128.

Bacmeister, J., P. J. Pegion, S. D. Schubert and M. J. Suarez, 2000: An atlas of seasonal means simulated by the NSIPP 1 atmospheric GCM. Vol 17. NASA Tech. Memo. 104606, Goddard Space Flight Center, Glennbelt, MD. 194 pp.

Campana, K. and P. Caplan, Editors 2005: Technical Procedure Bulletin for T382 Global Forecast System. (http://www.emc.ncep.noaa.gov/gc_wmb/Documentation/TPBoct05/T382.TPB.FINAL.html.

Dai A., K. E. Trenberth and T. R. Karl, 1998: Global variations in droughts and wet spells 1900-1995. *Geophy. Rev. Let.*, **25**, 3367-2962.

Dai A., K. E. Trenberth and T. Quin, 2004: A global dataset of Palmer Drought Severity Index for 1987-2002: Relationships with soil moisture and effects of surface warming. *J. Hydromet.*, **5**, 1117-1130.

Delworth and co-authors 2006: GFDL's CM2 global coupled climate models-Part 1: Formulation and simulation characteristics. *J. Climate*, **19**, 643-674.

Enfield, D. B., A. M. Mestas-Nunez and P. J. Trimble, 2001: The Atlantic multi decadal oscillation and its relation to rainfall and river flow over the U. S. *Geophy. Res. Let.* **28**, 2077-2080.

Hayes, M. J., M. D. Svoboda, D. A. Wilhite and O. V. Vanyarkho, 1999: Monitoring the 1996 drought using the standardized precipitation index. *Bull. Amer. Meteor.Soc.*, **80.** 429-438.

Higgins, R. W., W. Shi, E. Yarosh, and R. Joyce, 2000: Improved United States precipitation quality control system and analysis. NCEP/CPC Atlas 7, Climate Prediction Center, Camp Springs Md.

Hu, Q., and S. Feng, 2008: Variation of the North American summer monsoon regimes and the Atlantic multi decadal oscillations. *J. Climate*, **21**, 2371-2383.

Kiehl, J. T., J. J. Hack, G. Bonan, B. A. Boville, D. Williamson and P. Rasch, 1998: The National Center for Atmospheric Research Community Climate Model CCM3. *J. Climate*, **11**, 1131-1149.

Maurer, E. P., A. W. Wood, J. C. Adam, D. P. Lettenmaier, and B. Nijssen, 2002: A long term hydrologically based dataset of land surface fluxes and states for the conterminous United States. *J. Climate*, **15**, 3237-3251

McCabe, G. J., M. A. Palecki and J. L. Betancount, 2004: Pacific and Atlantic ocean influences on multi-decadal drought frequency in the United States. *Proc. Natl. Acad. Sci.* **101**, 4136-4141.

McKee, T. B., N. J. Doesken, and J. Kleist, 1993: The relationship of drought frequency and duration to time scales. Preprints, Eighth conf. on Applied Climatology. Anaheim Ca, AMS, 179-184.

McKee, T. B., N. J. Doesken, and J. Kleist, 1995: Drought monitoring with multiple time scales. Preprints, Nineth conf. on Applied Climatology. Dallas Tx, AMS, 233-236.

Mestas-Nunez, A., and D. B. Enfield, 1999: Rotated global modes of non ENSO Sea surface temperatura variability. *J. Climate* **12**, 2734-2746.

Milly, P. C. D., and A. B. Shmakin, 2002: Global modeling of land water and energy balances Part 1: The land dynamics (LaD) model. *J. Hydromet,* **3**,283-299.

Mo, K. C. 2008: Model based drought indices over the United States. *J. Hydromet.* In press.

Mo, K. C. and J. E. Schemm, 2008a : Drought and persistent wet spells over the United States and Mexico. *J. Climate*. **21**, 980-994.

Mo, K. C. and J. E. Schemm, 2008b : Relationships between ENSO and Drought over the Southeastern United States. *Geophy. Res. Let* **35**, doi:10.1029/ 2008GL034656.

Palmer, T. N and co-authors, 2004: Development of a European multimodel ensemble system for seasonal-interannual prediction (DEMETER). *Bull. Amer. Meteor. Soc.* **85**, 853-872.

Rogers, J. C., and J. S. M. Coleman 2003: Interactions between the Atlantic multi decadal oscillation, El Nino/La Nina and the PNA in winter Mississippi Valley stream flow. *Geophy. Res. Let.* Doi: 10.1029/2003GL017216.

Ropelewski, C. F., and M. S. Halpert, 1986: North American precipitation and temperature patterns associated with the El Nino/Southern Oscillation. *Mon. Wea. Rev.*, **114**, 2352-2362

------------, and ---------- ,1989: Precipitation patterns associated with the high index phase of the Southern Oscillation. *J. Climate*, **2**, 268-284.

Rowell, D. P. 1988: Assessing potential seasonal variability with an ensemble of multi decadal GCM simulation. *J. Climate* ,**11**,109-120.

Schubert S. D., M. J. Suarez, P. Pegion, R. D. Koster and J. T. Bacmeister, 2004: Causes of long term drought in the U. S. Great Plains. *J. Climate*, **17**, 485-503.

Schubert S. and the extended drought working group 2008: A USCLIVAR project to assess and compare the responses of global climate models to drought related SST forcing patterns: Overview and Results. *J. Climate*: Special USCLIVAR drought working group issue submitted.

Shukla. S., and A. W. Wood, 2008: Use of a standardized runoff index for characterizing hydrologic drought. *Geophy*. *Res.* *Let*. 35,doi:10.1029/2007GL032487.

Seager, R., Y. Kushnir, C. Herweijer, N. Naik and J. Velez, 2005: Modeling tropical forcing of persistent droughts and pluvials: 1862-2000. *J. Climate*, **18**, 4068-4091.

Smith, T. M., R. W. Reynolds, R. E. Livezey and D. C. Stokes, 1996: Reconstruction of historical sea surface temperatures using empirical orthogonal functions. *J. Climate*, **9,** 1403-1420.

Svoboda, M., D., and co-authors, 2002: The drought monitor. *Bull. Amer. Meteor. Soc.*, **83 ,** 1181-1190.

Figure captions

Fig. 1: (a) The Pacific SSTA pattern. Contour interval is 0.4 nondimensional units. Positive anomalies are shaded, (b) same as (a), but for the Atlantic SSTA pattern.

Fig.2: Composite of SPI 6 for January-March (JFM), (b) April-June (AMJ), (c) July-September (JAS) and October-December (OND). Contour interval is 0.4 with values between -0.8 and 0.8 omitted. Areas where positive (negative) anomalies are statistically significant at the 5% level based on the Monte Carlo test are shaded dark (light), (e)-(h) same as (a)-(d), but for P. Contour interval is 0.4 mm day^{-1}.

Fig.3: (a) Composite of SPI 6 for all seasons together. Contour interval is 0.4 with values between -0.8 and 0.8 omitted. Areas where positive (negative) anomalies are statistically significant at the 5% level based on the Monte Carlo test are shaded dark (light), (b) same as (a), but the composite of soil moisture anomalies. Contour interval is 15 mm. Values between -15mm and 15mm are omitted, and (c) same as (a), but for SRI6.

Fig.4: The frequency of drought occurrence *100 for (a) GFS, (b) GFDL, (c) NSIPP, and (d) CCM3 PwAn experiment. Contour interval is 5. Areas where values are statistically significant at the 5% level based on the Monte Carlo test are colored, (e)-(h) same as (a)-(d) but for the PcAn experiments.

Fig.5: The frequency of drought occurrence *100 from multi model ensemble for (a) PwAn, (b) PnAw, (c) PwAc, (d) PwAw, (e) PcAn, (f) PnAc, (g) PcAw and (h)

PcAc. Contour interval is 5. Areas where values are statistically significant at the 5% level based on the Monte Carlo test are shaded.

Fig.6: Mean precipitation anomaly averaged over the Great Plains (32-40^{o} N, 90-105^{o} W) for winter (red line), summer (green line) and annual (dark close circles) for the (a) PwAn GFS, (b) PcAn GFS, (c) PwAn NSIPP, (d) PcAn NSIPP, (e) PwAn GFDL, (f) PcAn GFDL, (g) PwAn CCM3 and (h) PcAn CCM3 experiment. (i)-(p) same as (a)-(h), but for the Southeast (32-40^{o} N, 75-80^{o} W over land).

Fig.7: Mean P anomaly difference averaged over the last 25 years of experiment integration between PwAn and PcAn for JFM for (a) GFS, (b) GFDL, (c) NSIPP and (d) CCM3 experiments. Contour interval is 0.2 mm day^{-1} Areas where positive (negative) anomalies are statistically significant at the 5% level based on the student t test by assuming one degree of freedom per year are shaded dark (light). (e)-(h) same as (a)-(d), but for JAS.

Fig.8: (a) The P difference between warm and cold decades of the AMO. Contour interval is 0.2 mm day^{-1} . Positive (negative) anomalies are shaded dark(light), (b) composite of SPI6 with all seasons together based on the RPC associated with Fig.1b. Contour interval is 0.2 mm day^{-1} Areas where positive (negative) anomalies are statistically significant at the 5% level based on the Monte Carlo test are shaded dark (light). (c) composite of SPI6 for cold ENSO based on the RPC associated with Fig.1a during the positive AMO decades. Contour interval is 0.4 mm day^{-1} Areas where positive (negative) anomalies are statistically significant at the 5% level based on the Monte Carlo test are

shaded dark (light). (d) same as (c), but for cold ENSO during the negative AMO decades, (e) same as (a), but for JAS, (f) same as (e), but for SPI6 with all seasons together, (g) same as (c), but for warm ENSO during the positive decades of the AMO and (h) same as (c), but for warm ENSO during the negative decades of the AMO.

Fig.9: The frequency of drought occurrence *100 for (a) GFS PcAc, (b) GFS PcAw, (c) GFDL PcAc, (d) GFDL PcAw, (e) NSIPP PcAc, (f) NSIPP PcAw, (g) CCM3 PcAc and (h) CCM3 PcAw experiment. Contour interval is 5. Areas where values are statistically significant at the 5% level based on the Monte Carlo test are shaded.

Fig.10: Composite of 200 hPa hight anomalies for (a) PnAc, (b) PcAw, (c) PcAn experiments for JFM for the GFS. Contour interval 10 m, Zero contours are omitted. Areas where values are statistically significant at the 5% level based on the Monte Carlo test are shaded, (d) composite of P anomalies for the PcAc experiment. Contour interval 0.2 mm day^{-1} (e) same as (a), but for PcAc experiment, (f) same as (a), but for PnAw experiment, (g) same as (a), but for PwAc experiment and (h) same as (d), but for PcAw experiment.

Figure 1

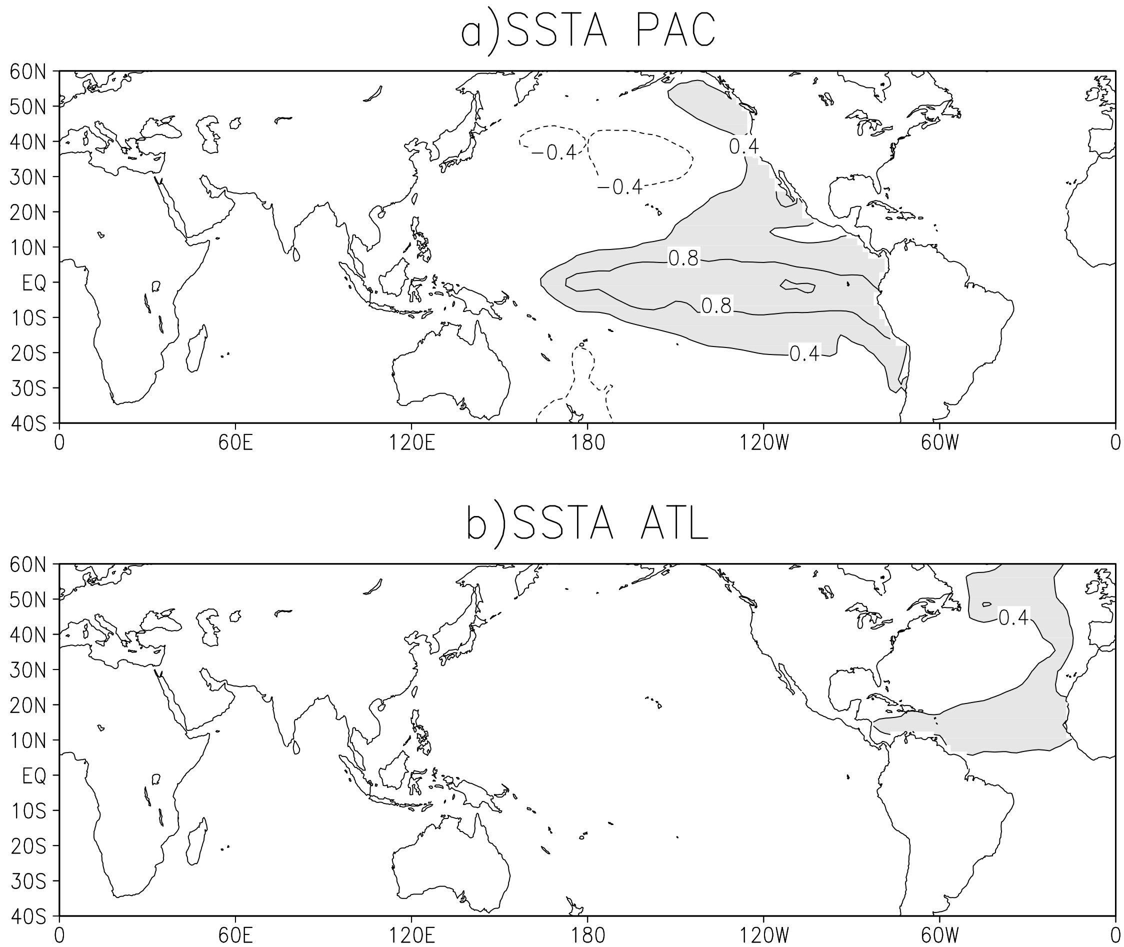

Fig. 1: (a) The Pacific SSTA pattern. Contour interval is 0.4 nondimensional units. Positive anomalies are shaded, (b) same as (a), but for the Atlantic SSTA pattern.

Figure 2

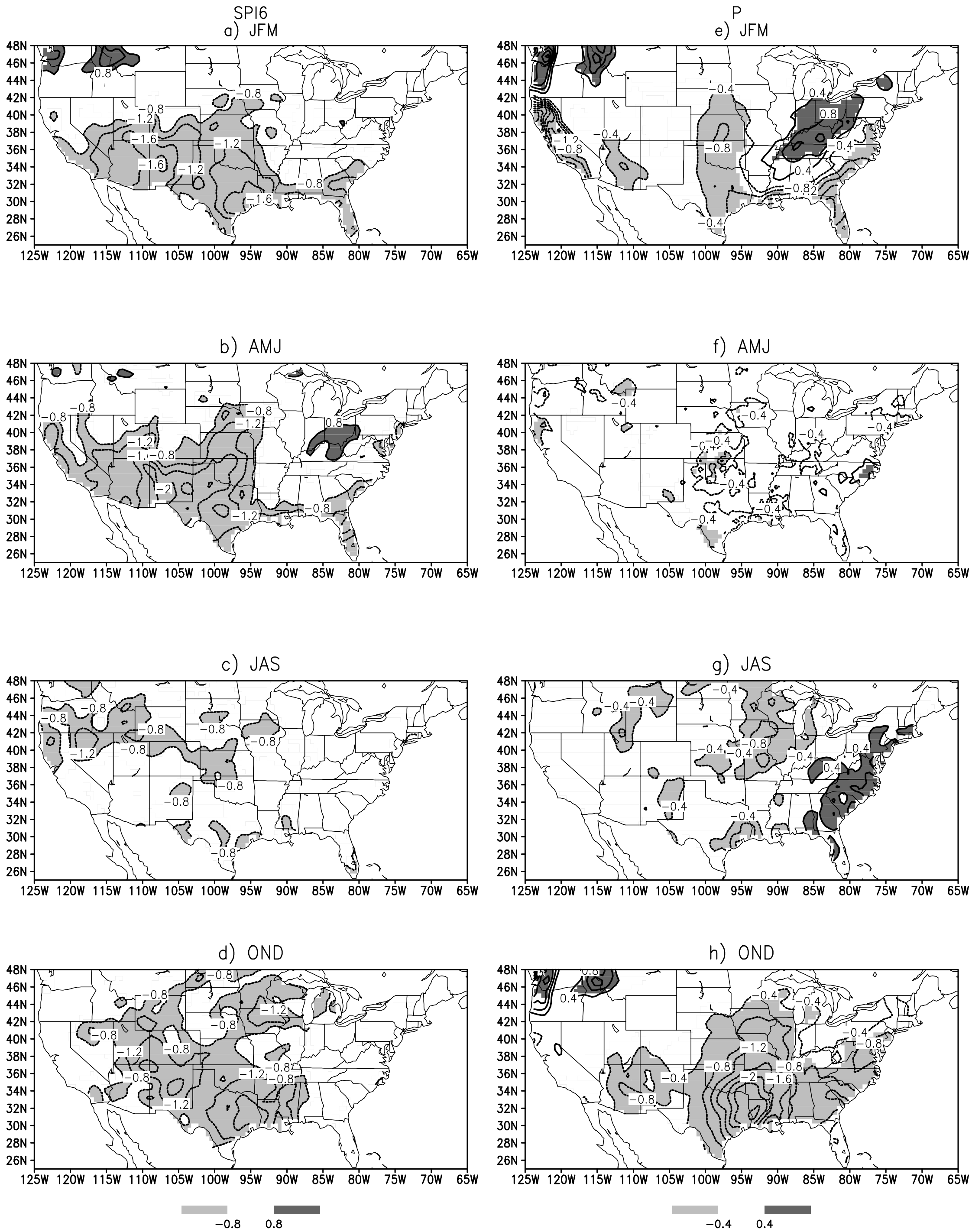

Fig.2: Composite of SPI 6 for January-March (JFM), (b) April-June (AMJ), (c) July-September (JAS) and October-December (OND). Contour interval is 0.4 with values between -0.8 and 0.8 omitted. Areas where positive (negative) anomalies are statistically significant at the 5% level based on the Monte Carlo test are shaded dark (light), (e)-(h) same as (a)-(d), but for P. Contour interval is 0.4 mm day^{-1}.

Figure 3

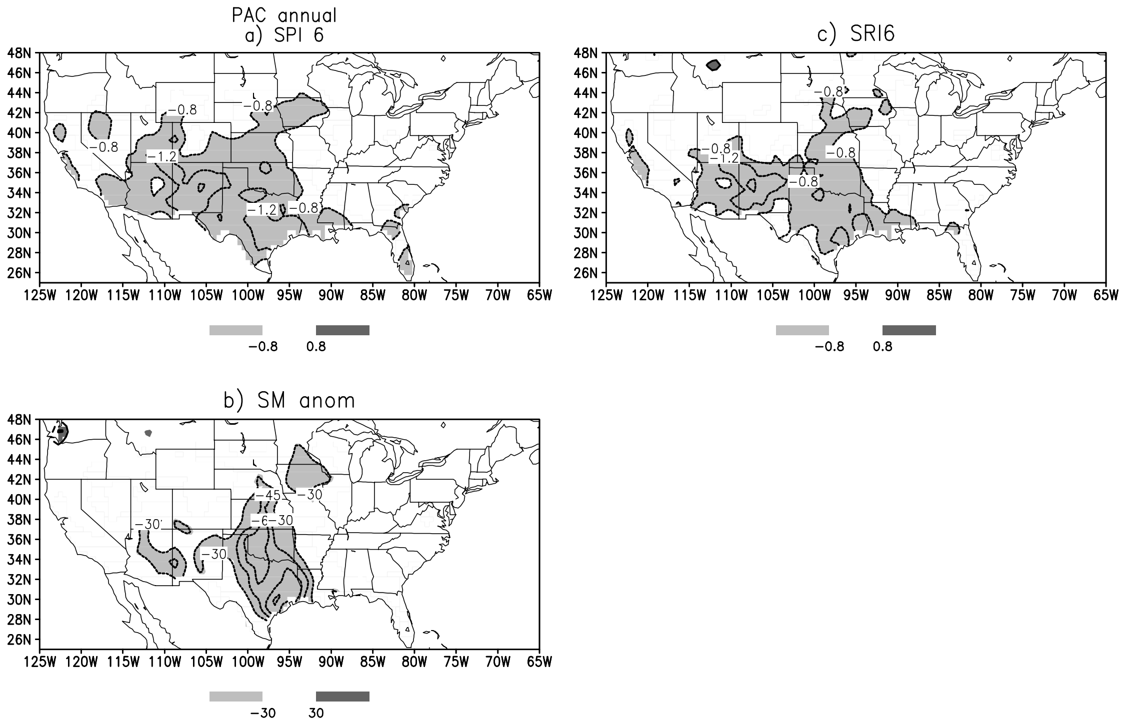

Fig.3: (a) Composite of SPI 6 for all seasons together. Contour interval is 0.4 with values between -0.8 and 0.8 omitted. Areas where positive (negative) anomalies are statistically significant at the 5% level based on the Monte Carlo test are shaded dark (light), (b) same as (a), but the composite of soil moisture anomalies. Contour interval is 15 mm with values between -15 and 15 mm omitted, and (c) same as (a), but for SRI6.

Figure 4

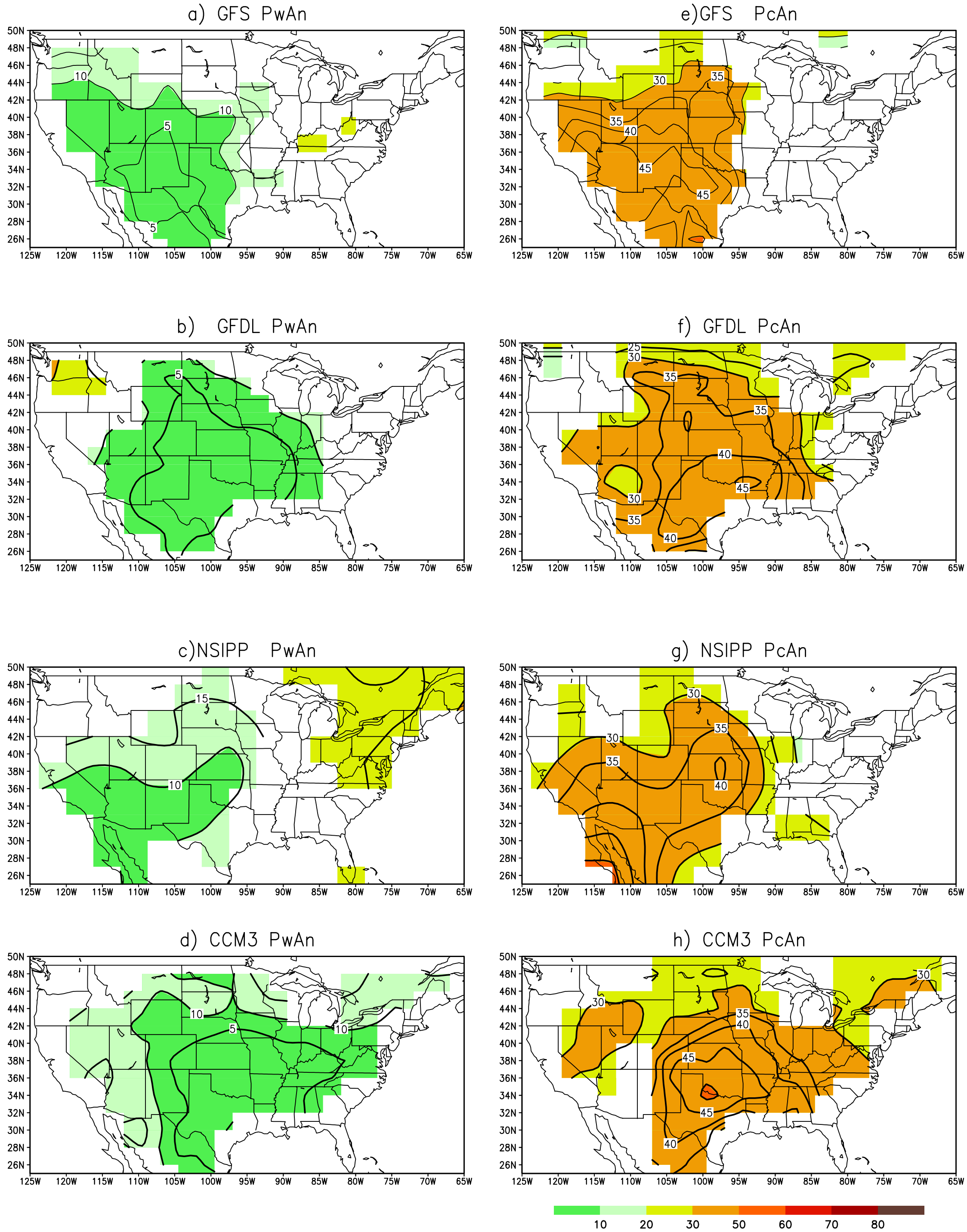

Fig.4: The frequency of drought occurrence *100 for (a) GFS, (b) GFDL, (c) NSIPP, and (d) CCM3 PwAn experiment. Contour interval is 5. Areas where values are statistically significant at the 5% level based on the Monte Carlo test are shaded. (e)-(h) same as (a)-(d) but for the PcAn experiments.

Figure 5

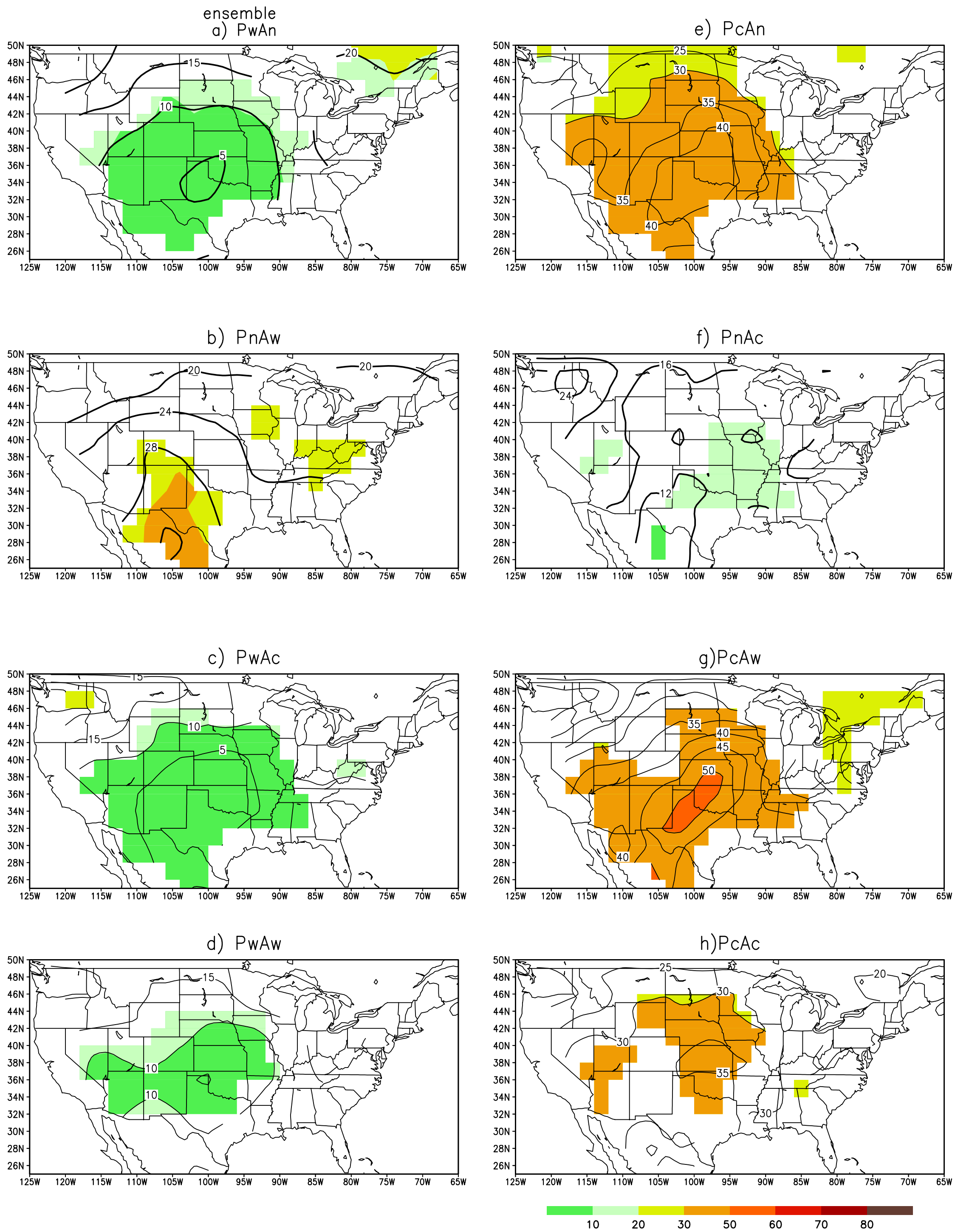

Fig.5: The frequency of drought occurrence *100 from multi model ensemble for (a) PwAn, (b) PnAw, (c) PwAc, (d) PwAw, (e) PcAn, (f) PnAc, (g) PcAw and (h) PcAc. Contour interval is 5. Areas where values are statistically significant at the 5% level based on the Monte Carlo test are shaded.

Figure 6

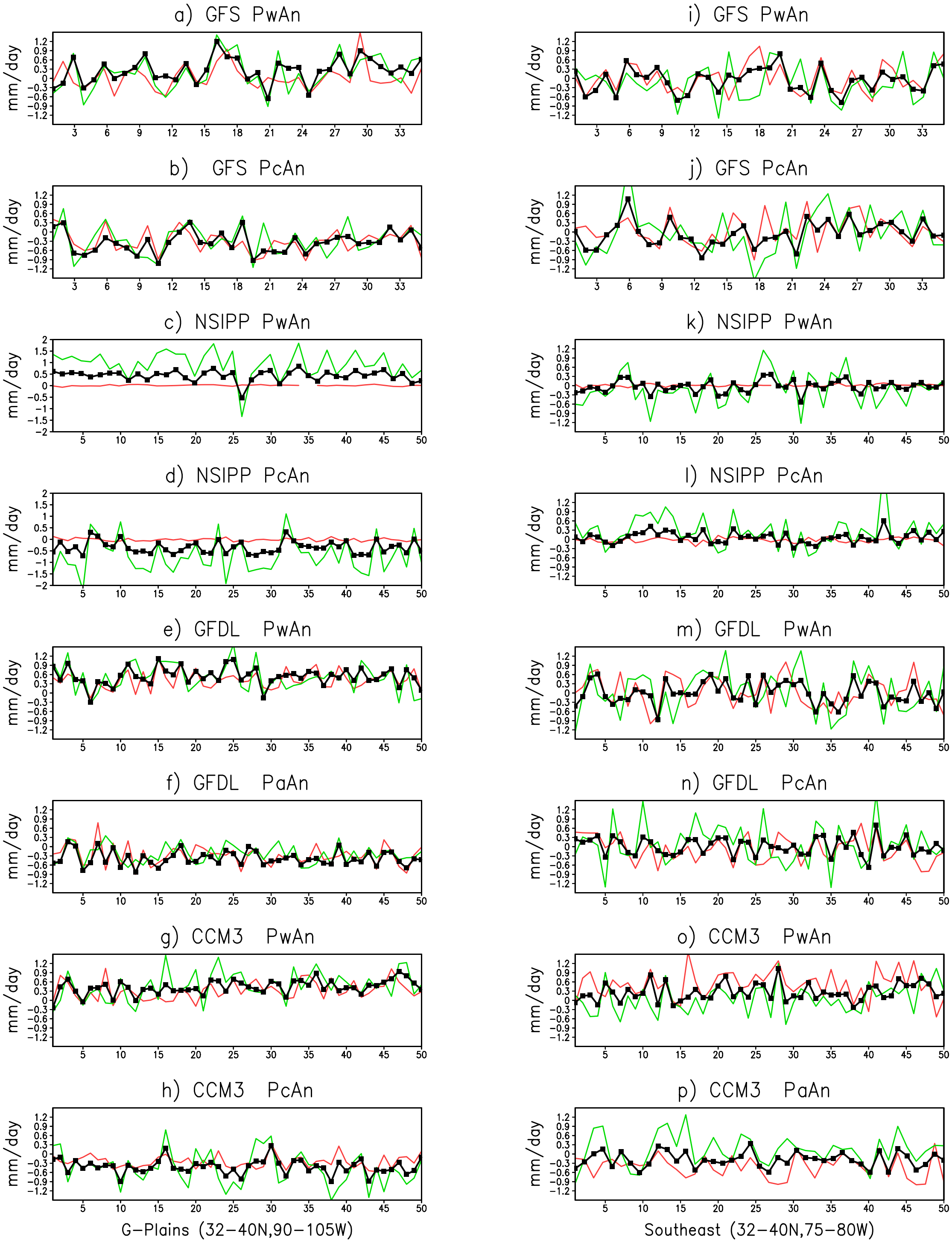

Fig.6: Mean precipitation anomaly averaged over the Great Plains (32-40° N, 90-105 ° W) for winter (red line), summer (green line) and annual (dark close circles) for the (a) PwAn GFS, (b) PcAn GFS, (c) PwAn NSIPP, (d) PcAn NSIPP, (e) PwAn GFDL, (f) PcAn GFDL, (g) PwAn CCM3 and (h) PcAn CCM3 experiment. (i)-(p) same as (a)-(h), but for the Southeast (32-40 ° N, 75-80 ° W over land).

Figure 7

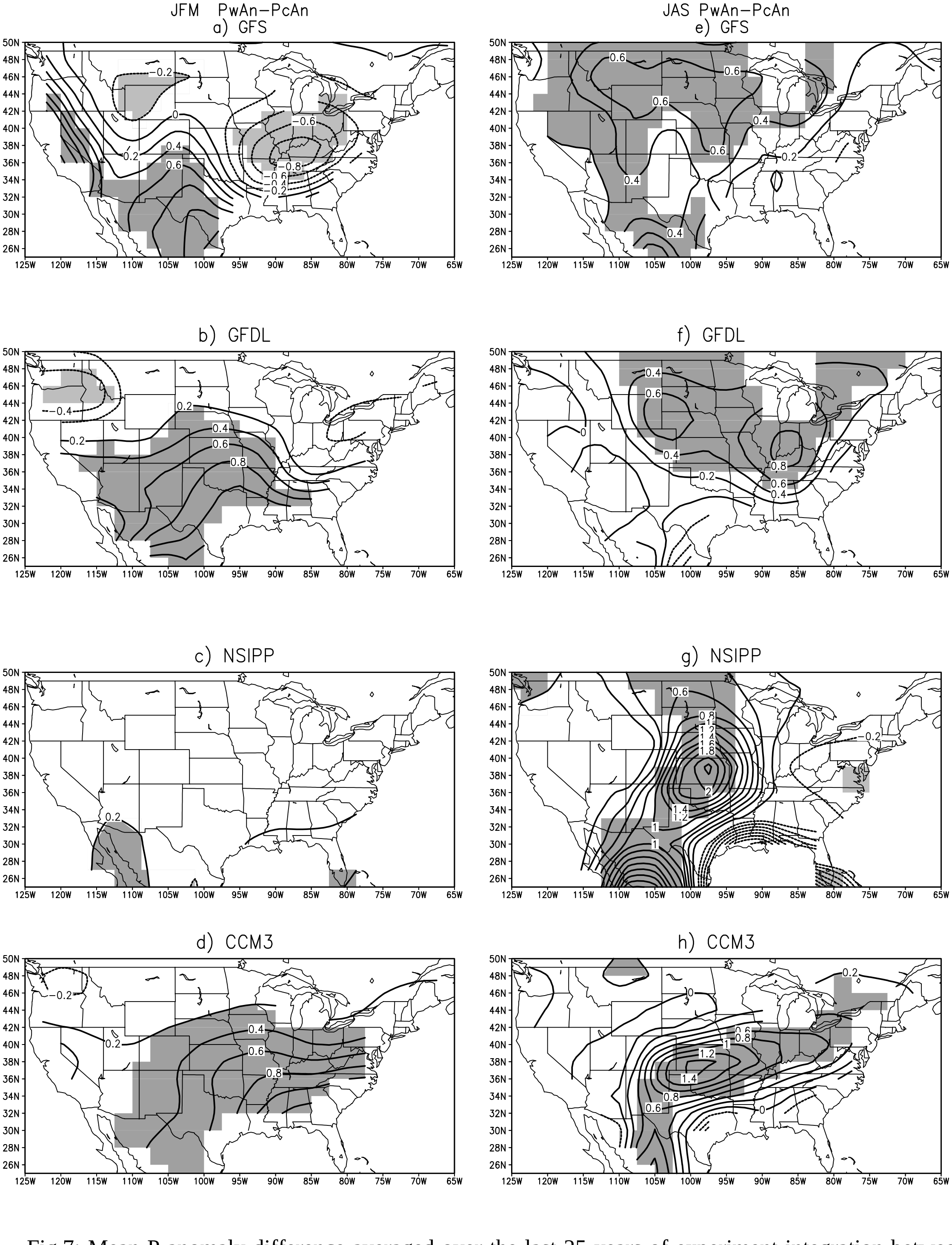

Fig.7: Mean P anomaly difference averaged over the last 25 years of experiment integration between PwAn and PcAn for JFM for (a) GFS, (b) GFDL, (c) NSIPP and (d) CCM3 experiments. Contour interval is 0.2 mm day^{-1} Areas where positive (negative) anomalies are statistically significant at the 5% level based on the student t test by assuming one degree of freedom per year are shaded dark (light). (e)-(h) same as (a)-(d), but for JAS.

Figure 8

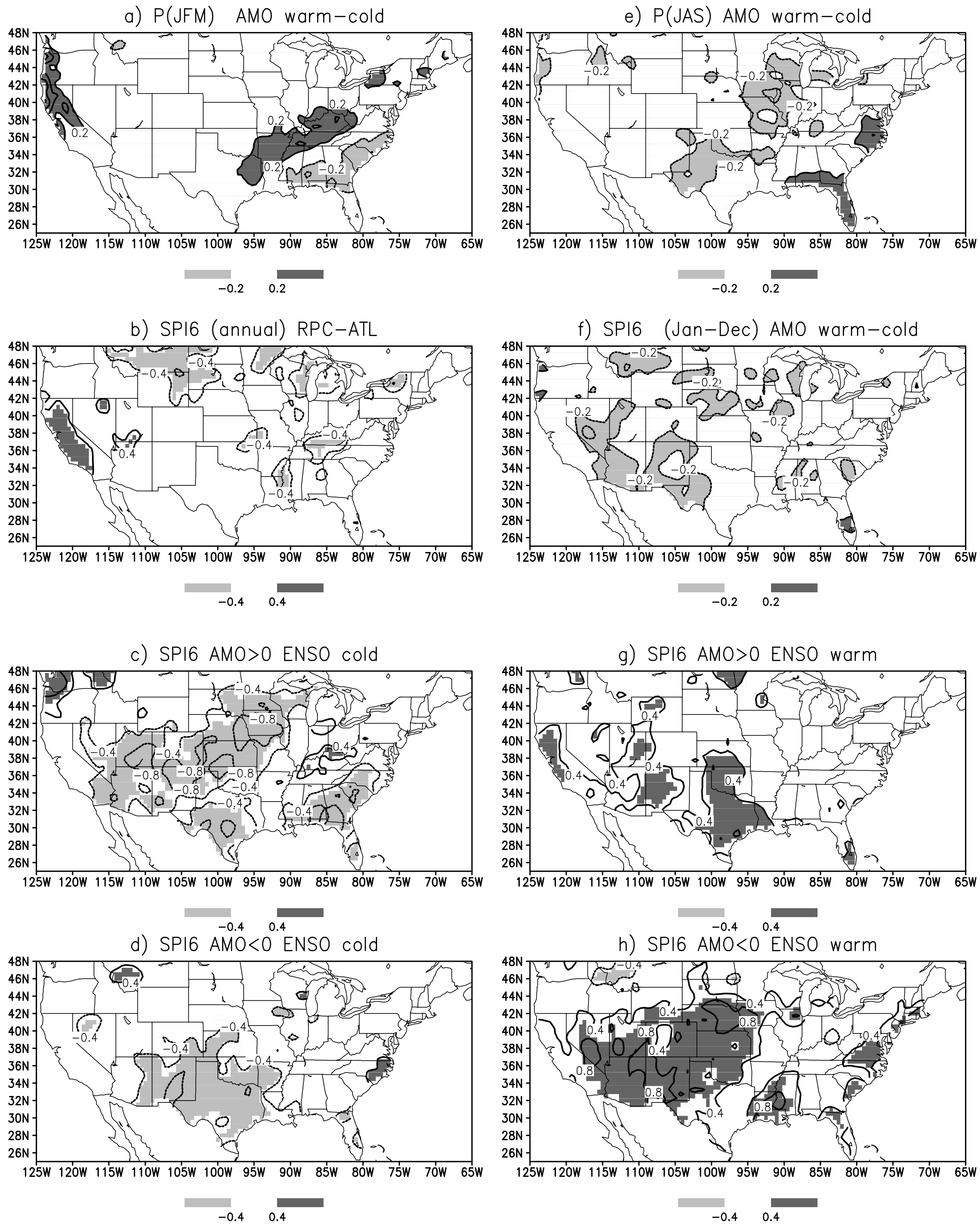

Fig.8: (a) The P difference between warm and cold decades of the AMO. Contour interval is 0.2 mm day^{-1} . Positive (negative) anomalies are shaded dark(light), (b) composite of SPI6 with all seasons together based on the RPC associated with Fig.1b. Contour interval is 0.2 mm day^{-1} Areas where positive (negative) anomalies are statistically significant at the 5% level based on the Monte Carlo test are shaded dark (light). (c) composite of SPI6 for cold ENSO based on the RPC associated with Fig.1a during the positive AMO decades. Contour interval is 0.4 mm day^{-1} Areas where positive (negative) anomalies are statistically significant at the 5% level based on the Monte Carlo test are shaded dark (light). (d) same as (a), but for cold ENSO during the negative AMO decades, (e) same as (a), but for JAS, (f) same as (e), but for SPI6 with all seasons together, (g) same as (c), but for warm ENSO during the positive decades of the AMO and (h) same as (c), but for warm ENSO during the negative decades of the AMO.

Figure 9

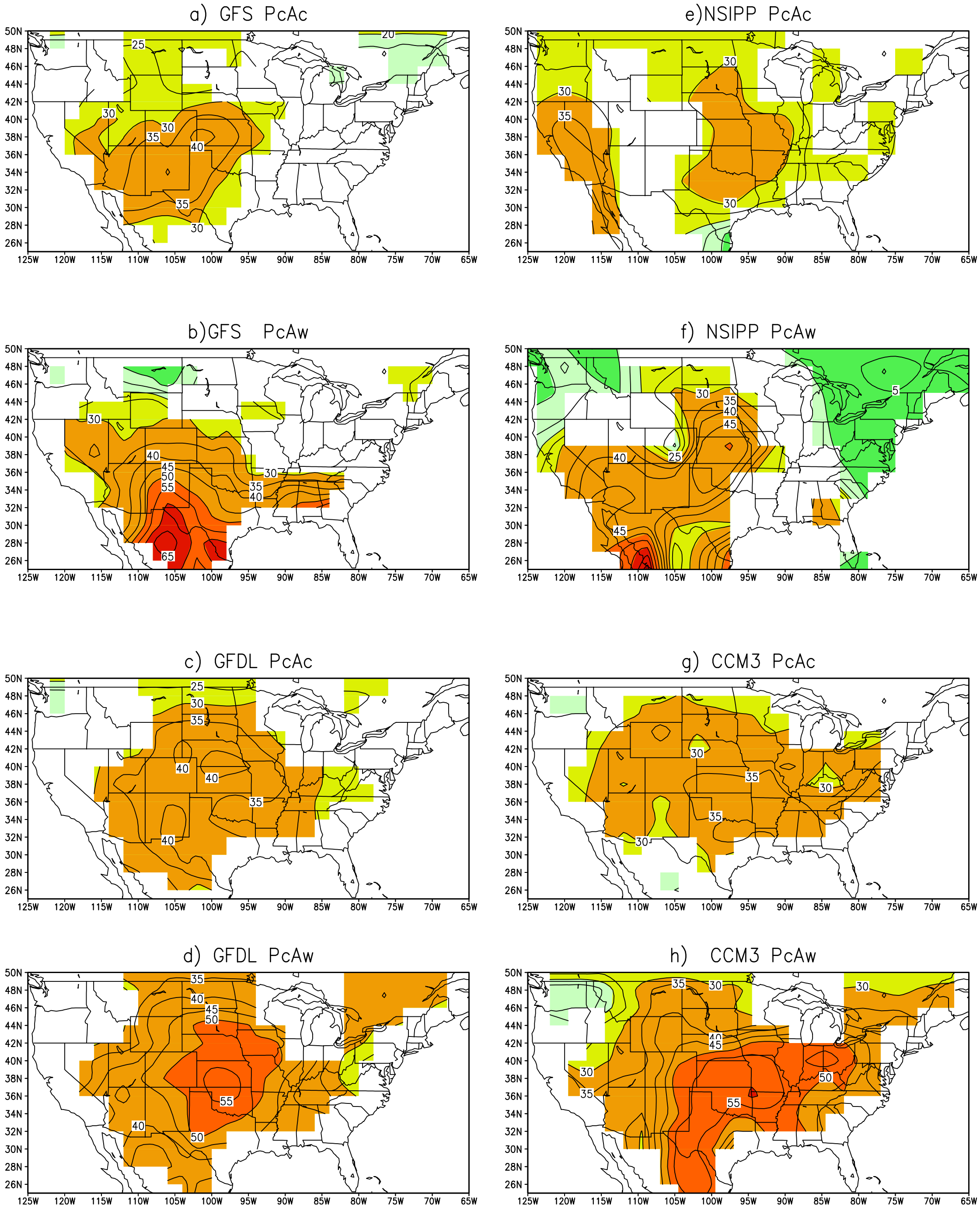

Fig.9: The frequency of drought occurrence *100 for (a) GFS PcAc, (b) GFS PcAw, (c) GFDL PcAa, (d) GFDL PcAw, (e) NSIPP PcAc, (f) NSIPP PcAw, (g) CCM3 PcAc and (h) CCM3 PcAw experiment. Contour interval is 5. Areas where values are statistically significant at the 5% level based on the Monte Carlo test are shaded.

Figure 10

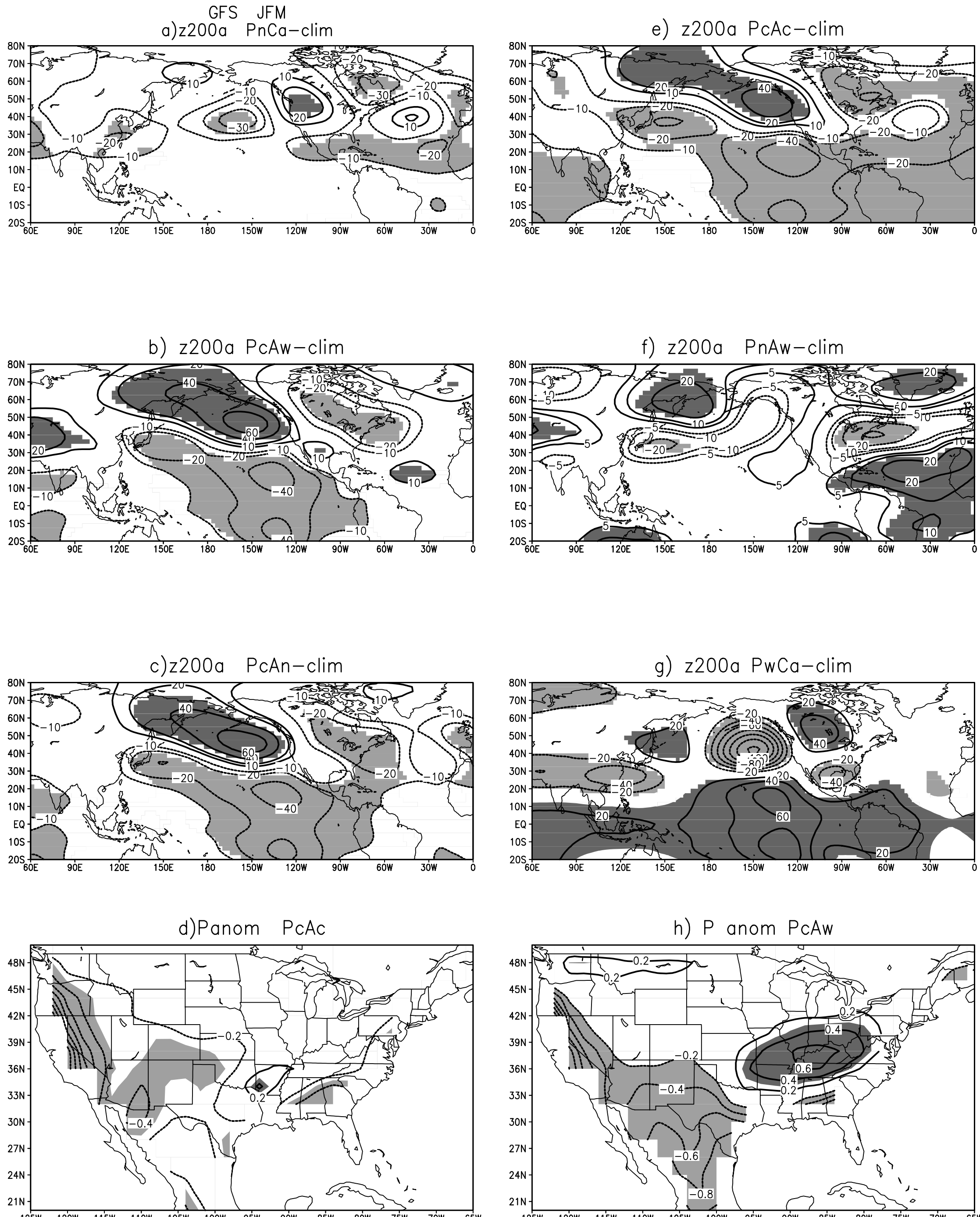

Fig.10: Composite of 200 hPa hight anomalies for (a) PnAc, (b) PcAw, (c) PcAn experiments for JFM for the GFS. Contour interval 10 m, Zero contours are omitted. Areas where values are statistically significant at the 5% level based on the Monte Carlo test are shaded, (d) same as (c), but for P anomalies. Contour interval 0.2 mm day^{-1} (e) same as (a), but for PcAc experiment, (f) same as (a), but for PnAw experiment, (g) same as (a), but for PwAc experiment and (h) same as (d), but for PcAw experiment.